JMEPEG (2008) 17:465–471
DOI: 10.1007/s11665-007-9188-y

1059-9495/$19.00

Optimization of Compositional and Technological Parameters for Phosphate Graphite Sand

An-hui Cai, Hua Chen, Jing-ying Tan, Min Chen, Xiao-song Li, Yong Zhou, and Wei-ke An

(Submitted February 4, 2007; in revised form October 28, 2007)

In present work, the compression strength and tensile strength of phosphate graphite sand with compositional and technological parameters (phosphoric acid, Al_2O_3, drying temperature, and drying time) were experimentally investigated. An L_9 (3^4) orthogonal array was employed to analyze the effect of these four parameters on the compression strength and tensile strength, respectively. In addition, the radial basis function artificial neural network (RBFANN) was used to establish the models for compression strength and tensile strength, respectively. Moreover, the simulation and prediction results by the RBFANN and linear and non-linear regressions are compared. The results are as follows: the optimum scheme for phosphate graphite sand designed by us is phosphoric acid 24%, Al_2O_3 30%, drying temperature 400 °C, and drying time 60 min. The ascending sequence of the effect of four factors on both compression strength and tensile strength of phosphate graphite sand is drying time, drying temperature, Al_2O_3, and phosphoric acid. In addition, the prediction and simulation results show that RBFANN outperforms Taguchi approach for modeling.

Keywords artificial neural network, optimization, orthogonal design, phosphate graphite sand

1. Introduction

The graphite mold has been applied to obtain high-quality castings (Ref 1-3) because it possesses such performances as high heat conductivity (116.3-127.9 Wm^{-1} K^{-1}) (Ref 2) and coefficient of temperature conductivity which leads to high chilling effect, high melting temperature and high strength, better heat resistance capacity and non-deformability, low linear expansion factor ($0.5\text{-}4.0\times10^{-6}$/°C) (Ref 2), better suitability and low cost. As shown in (Ref 1), heat conductivity and coefficient of temperature conductivity of graphite mold are 2-3 and 3-4 times more than those of sand mold, respectively. The microstructure of Al-based alloy (ZL101) casting by graphite mold is greatly refined, the pinhole and the porosity defect in Al-castings are effectively eliminated, resulting in the increase of 15.4% for tensile strength and 25.8% for extension percentage. Pan (Ref 3) successfully prepared Al_2O_3-Cr and Al_2O_3-(Cr_2O_3)-Cr ceramic matrix composites in ceramic mold and graphite mold by combustion synthesis. The uniformity and fineness of microstructure of the composites in graphite mold are superior to those obtained in a ceramic mold. Therefore, it is important to research the performance of phosphate graphite sand.

A. Cai, Hua Chen, J. Tan, X. Li, Yong Zhou, and **W. An**, Department of Mechanical and Electrical Engineering, Hunan Institute of Science and Technology, YueYang 414000, P.R. China; and **Min Chen**, Department of Physical and Electronic Engineering, Hunan Institute of Science and Technology, YueYang 414000, P.R. China. Contact e-mail: cah1970@sohu.com.

The orthogonal design and artificial neural network modeling technique are two main methods for material design and evaluation. Orthogonal design is a method for test design aiming to multifactor and multilevel based on orthogonal theory. Since it presents equilibrium distribution and regular comparability, the optimum scheme can be rapidly obtained by analysis of variance, largely reducing testing numbers, shortening test time, and minimizing cost. And it has been applied to optimize material's composition, production technology, management and distribution, etc. (Ref 4-8). For example, Bagci and Aykut (Ref 6) discussed an application of the Taguchi method for investigating the effects of cutting parameters on the surface roughness value in the face milling of stellite 6 material. In addition, Tsao (Ref 8) investigated the thrust force and surface roughness of core drill with drill parameters (grit size of diamond, thickness, feed rate, and spindle speed) in drilling carbon fiber reinforced plastic (CFRP) laminate by an orthogonal array.

Artificial neural networks have received extensive attention because of their self-adaptive, self-organization, and self-study. It is well known that they can solve many practical problems as pattern recognition, function approximation, system identification, time series forecasting, etc. (Ref 9-16). For example, Shie (Ref 9) optimized dry machining parameters for high-purity graphite in end-milling process by an artificial neural network and the sequential quadratic programming method. The results showed that this algorithm yielded better performance than the traditional methods such as the Taguchi method and the design of experiments approach. Sheikh-Ahmand and Twomey (Ref 10) developed an artificial neural network model for high strain-rate deformation of Al 7075-T6 based on flow data found in the literature and orthogonal machining tests and the ANN predictions were shown to be superior to a parametric constitutive model.

The aims of this article are to obtain optimum compositional and technological parameters for phosphate graphite sand and compare the differences between afore-mentioned two methods.

2. Experimental

2.1 Experimental Procedures

After the graphite powder (2-3 mm) and Al_2O_3 powder (wt.95%, 1 mm) were dry mixed 5 min in QS114 sand mixer, the mixture of graphite and Al_2O_3 powder was mixed 10 min by adding the mixture whose ratio of 1:1 (wt.%) for water and phosphoric acid (wt.85%). And then, the wet mixture was made into three $\Phi 50 \times 50$ mm standard samples for compression strength test and three "8" shaped standard samples (shown in Fig. 1) for tensile strength test by XYD-1 molding machine under 0.2 MPa (±0.01 MPa). Finally, these samples were dried in SX2-12-10 resistance furnace (±1 °C). The compression and tensile tests were performed on SQY hydraulic strength-testing machine (±0.01 MPa) and XQY-II intelligence sand strength-testing machine (±0.01 MPa), respectively.

2.2 Experimental Plan

For the elaboration of experimental plan, the orthogonal method for four factors at three levels was adopted. In Table 1, the factors to be studied and the assignment of the corresponding levels are indicated. The chosen array was the L_9 (3^4) which has nine rows corresponding to the number of tests (8 degrees of freedom) with four columns at three levels, as shown in Table 2. The factors are assigned to the columns. The plan of experiments is made of nine tests (array rows) in which the first column was assigned to phosphoric acid (*A*), the second column to the Al_2O_3 (*B*), the third column to the drying temperature (*C*), and the forth column to the drying time (*D*), respectively. The experimental results for the compression strength and tensile strength are shown in Table 2.

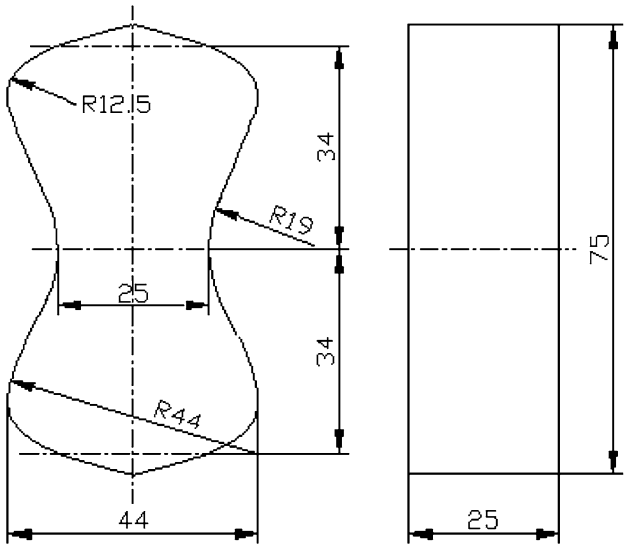

Fig. 1 Schematic diagram of the sample for tensile strength

Table 1 Assignment of the levels to the factors

Level	Phosphoric acid, *A*, wt.%	Al_2O_3, *B*, wt.%	Drying temperature, *C*, °C	Drying time, *D*, min
1	18	16	400	40
2	21	18	500	60
3	24	30	600	80

3. Results and Analyses

3.1 Orthogonal Design

An analysis of variance of the data was done with the compression strength and the tensile strength for analyzing the influence of the phosphoric acid, Al_2O_3, drying temperature and drying time of the contact on the total variance of the results, respectively. Tables 3 and 4 show the results of the analysis of variance with the compression strength and the tensile strength, respectively. The last column of Tables 3 and 4 shows the percentage of contribution (P) on the total variation indicating the degree of influence on the result. From the analysis of Tables 3 and 4, one can observe that the ascending sequences of influence of four factors on compression strength and tensile strength both are drying time, drying temperature, Al_2O_3, and phosphoric acid. In addition, the

Table 2 Orthogonal array L_9 (3^4) and experimental results

Exp. no.	*A*	*B*	*C*	*D*	Compression strength, MPa	Tensile strength, MPa
1	1	1	1	1	0.91	0.08
2	2	1	2	2	0.57	0.13
3	3	1	3	3	1.27	0.24
4	1	2	2	3	0.90	0.19
5	2	2	3	1	0.48	0.30
6	3	2	1	2	1.08	0.23
7	1	3	3	2	0.65	0.18
8	2	3	1	3	1.29	0.21
9	3	3	2	1	2.22	0.47

Table 3 Analysis of variance for compression test

Source of variance	Squared deviations	Degrees of freedom	Variances	P, %
A	1.0488	2	0.5244	47.0
B	0.5514	2	0.2757	24.7
C	0.3427	2	0.1714	15.3
D	0.2896	2	0.1448	13.0
Total	2.2325	8	–	100

Table 4 Analysis of variance for tensile test

Source of variance	Squared deviations	Degrees of freedom	Variances	P, %
A	0.0407	2	0.0204	40.9
B	0.0289	2	0.0145	29.1
C	0.0167	2	0.0084	16.8
D	0.0131	2	0.0066	13.2
Total	0.0994	8	–	100

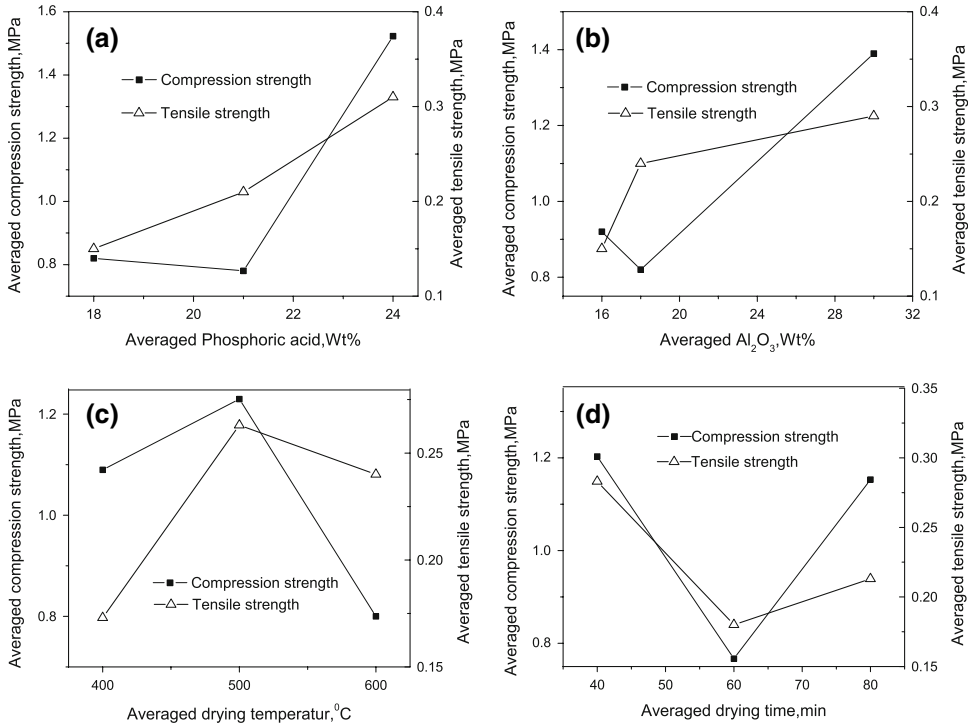

Fig. 2 Effects of four factors on the compression strength and the tensile strength

averaged values of compression strength and tensile strength for each parameter at different levels are plotted in Fig. 2. It is clear from Fig. 2 that the compression strength and the tensile strength are both maximums at the third level of parameter A (A_3) and parameter B (B_3), the second level of parameter C (C_2) and the first level of D (D_1). It indicates that the optimum combinations of four factors for the compression strength and tension strength both are $A_3B_3C_2D_1$. Therefore, the theoretical optimum values are in agreement with the values of test 9, i.e., 2.22 MPa for the compression strength and 0.47 MPa for tensile strength, respectively. It indicates that the test 9 is the optimum test for both the compression strength and tensile strength. On the other hand, the correlations between four factors (phosphoric acid, Al_2O_3, drying temperature, and drying time) and the measured parameters (compression strength σ_c and tensile strength σ_t) can be obtained by multiple linear and quadratic regressions, respectively. The equations are as follows:

$$\sigma_c = 0.1172A + 3.833 \times 10^{-2}B - 1.467 \times 10^{-3}C - 1.25 \times 10^{3}D - 1.43,\ R = 0.79 \quad \text{(Eq 1)}$$

$$\sigma_t = 2.722 \times 10^{-2}A + 7.713 \times 10^{-3}B + 3.333 \times 10^{-4}C - 1.75 \times 10^{-3}D - 0.5723,\ R = 0.87 \quad \text{(Eq 2)}$$

$$\sigma_c = 17.469 - 1.7106A - 0.2804B + 2.6867 \times 10^{-2}C - 0.12475D + 4.3519 \times 10^{-2}A^2 + 6.8254 \times 10^{-3}B^2 - 2.8333 \times 10^{-5}C^2 + 1.0292 \times 10^{-3}D^2,\ R = 1 \quad \text{(Eq 3)}$$

$$\sigma_t = -5.833 \times 10^{-2}A + 0.14484B + 6 \times 10^{-3}C - 2.225 \times 10^{-2}D + 2.037 \times 10^{-3}A^2 - 2.94 \times 10^{-3}B^2 - 5.6667 \times 10^{-6}C^2 + 1.71 \times 10^{-4}D^2 - 1.97233,\ R = 1 \quad \text{(Eq 4)}$$

In order to examine the fitted effect of Eq 1-4, the root-mean-square errors (RMSE) analysis (Ref 9) for the compression strength and tensile strength predicted by Eq 1-4 in the orthogonal array are adopted. Tables 5 and 6 show the comparative results between the linear regression and quadratic regression for the compression strength and tensile strength, respectively. In Table 5, the RMSEs of the compression strength for Eq 1 and 3 are 0.3007 and 0.0005, respectively. In Table 6, the RMSEs of the tensile strength for Eq 2 and 4 are 0.0516 and 0, respectively. It indicates that Eq 1 and 2 do not correlate the evolution of the compression strength and the tensile strength with the phosphoric acid, Al_2O_3, drying temperature and drying time, and the quadratic regression outperforms the linear regression.

3.2 Artificial Neural Network Method

It is well-known that artificial neural network ANN can extract usable information from large quantity of discrete data with noise and is suitable for resolving the highly non-linear and uncertain problems (Ref 13-16).

In general, there are two kinds of ANN, i.e., back-propagation artificial neural network BPANN and radial basis function artificial neural network RBFANN, for being used to establish the model of the prediction. Although the BPANN has stronger generalization capacity, it is difficult to select its

training parameters such as learning rate, initial weight, and objective error, and the structure parameters such as the number of hidden layers and the number of neurons in hidden layer. In addition, the training procedure is time-consuming. However, the RBFANN is easy to use and its training procedure is rapid, though its generalization capacity is worse than that of BPANN. In this section, the aim is to construct the RBFANN model whose samples are the values of orthogonal arrays in Table 2 and research the performance of the RBFANN model. We established two RBFANN models with four inputs (phosphoric acid, Al_2O_3, drying temperature, and drying time) and one output (either compression strength or tensile strength) for the prediction of compression strength and tensile strength, respectively. Nine sets of data conforming to L_9 (3^4) design have been procured and the outputs and inputs are normalized by Eq 5 to improve the training efficiency.

$$x' = 0.1 + 0.8\frac{x - x_{\min}}{x_{\max} - x_{\min}} \quad \text{(Eq 5)}$$

where, x' is the normalized value of x, x is initial value of one of afore-mentioned outputs and inputs, $x_{\max}$ and $x_{\min}$ are the maximum and minimum of x, respectively.

It is important to select a suitable distribution parameter t, which is a unique parameter during the training, in order to obtain reliable RBFANN models for the compression strength and tensile strength, respectively. According to the experience, the parameter $t = 2$ is selected for both the compression strength and tensile strength. After the RBFANN model has been obtained, the adequacy of the model should be inspected to confirm that the RBFANN model has extracted all relevant information from the experimental data. The RMSE analysis (Ref 9) is adopted. The RMSEs for the compression strength and

Table 5 Comparison for the compression strength σ_c (MPa) by the RBFANN, Eq 1 and 3

Exp. no	*A*	*B*	*C*	*D*	Actual σ_c	Predicted σ_c by RBFANN	RBFANN residual	Predicted σ_c by Eq 1	Eq 1 residual	Predicted σ_c by Eq 3	Eq 3 residual
1	1	1	1	1	0.91	0.91	0	0.6561	0.2539	0.9095	–0.0005
2	2	1	2	2	0.57	0.57	0	0.8360	–0.2660	0.5696	–0.0004
3	3	1	3	3	1.27	1.27	0	1.0159	0.2541	1.2696	–0.0004
4	1	2	2	3	0.90	0.90	0	0.5360	0.3640	0.8997	–0.0003
5	2	2	3	1	0.48	0.48	0	0.7909	–0.3109	0.4795	–0.0005
6	3	2	1	2	1.08	1.08	0	1.4109	–0.3309	1.0794	–0.0006
7	1	3	3	2	0.65	0.65	0	0.8743	–0.2243	0.6497	–0.0003
8	2	3	1	3	1.29	1.29	0	1.4943	–0.2043	1.2895	–0.0005
9	3	3	2	1	2.22	2.22	0	1.7492	0.4280	2.2194	–0.0006
						RMS error by RBFANN	0	RMS error by Eq 1	0.3007	RMS error by Eq 3	0.0005

Table 6 Comparison for the tensile strength σ_t (MPa) by the RBFANN, Eq 2 and 4

Exp. no	*A*	*B*	*C*	*D*	Actual σ_t	Predicted σ_t by RBFANN	RBFANN residual	Predicted σ_t by Eq 2	Eq 2 residual	Predicted σ_t by Eq 4	Eq 4 residual
1	1	1	1	1	0.08	0.08	0	0.1044	–0.0244	0.08	0
2	2	1	2	2	0.13	0.13	0	0.1844	–0.0544	0.13	0
3	3	1	3	3	0.24	0.24	0	0.2644	–0.0244	0.24	0
4	1	2	2	3	0.19	0.19	0	0.0831	0.1069	0.19	0
5	2	2	3	1	0.30	0.30	0	0.2681	0.0319	0.30	0
6	3	2	1	2	0.23	0.23	0	0.2481	–0.0159	0.23	0
7	1	3	3	2	0.18	0.18	0	0.2440	–0.064	0.18	0
8	2	3	1	3	0.21	0.21	0	0.2240	–0.0140	0.21	0
9	3	3	2	1	0.47	0.47	0	0.4090	0.0610	0.47	0
						RMS error by RBFANN	0	RMS error by Eq 2	0.0516	RMS error by Eq 4	0

Table 7 Results of the examination test data and the predictions by RBFANN

					Compression strength, MPa			Tensile strength, MPa		
Exp. no	*A*	*B*	*C*	*D*	RBFANN	Actual	Error, %	RBFANN	Actual	Error, %
1c	18	16	500	60	0.5420	0.54	0.37	0.1278	0.13	–1.69
2c	24	18	400	80	0.9257	0.92	0.62	0.2180	0.22	–0.91
3c	21	30	600	60	1.2158	1.22	–0.34	0.2398	0.24	–0.08
4c	18	16	500	80	0.8861	0.89	–0.44	0.2258	0.23	–1.83
5c	21	30	400	60	1.5316	1.53	0.10	0.1873	0.18	4.06
6c	24	18	600	40	1.1475	1.14	0.66	0.4535	0.46	–1.41

tensile strength are shown in Tables 5 and 6, respectively. In Tables 5 and 6, the RMES of the compression strength and tensile strength for the RBFANN both are 0. It indicates that the RBFANN models for the compression strength and tensile strength are both adequate. Furthermore, by investigating the prediction capacity of RBFANN model, other six tests are performed. Table 7 shows these six examination test data and the corresponding values predicted by RBFANN models, respectively. In addition, Fig. 3 shows the linear correlation coefficients, R, which measure the strength of a linear relationship between the experimental data and the RBFANN predicted values. As shown in Table 7, it is found that the maximum errors are 4.06% for tension strength and 0.66% for compression strength, respectively. At the same time, in Fig. 3, the correlation coefficients are 0.9999 for the compression strength and 0.9994 for the tensile strength, respectively. It indicates that the RBFANN models are rather effective.

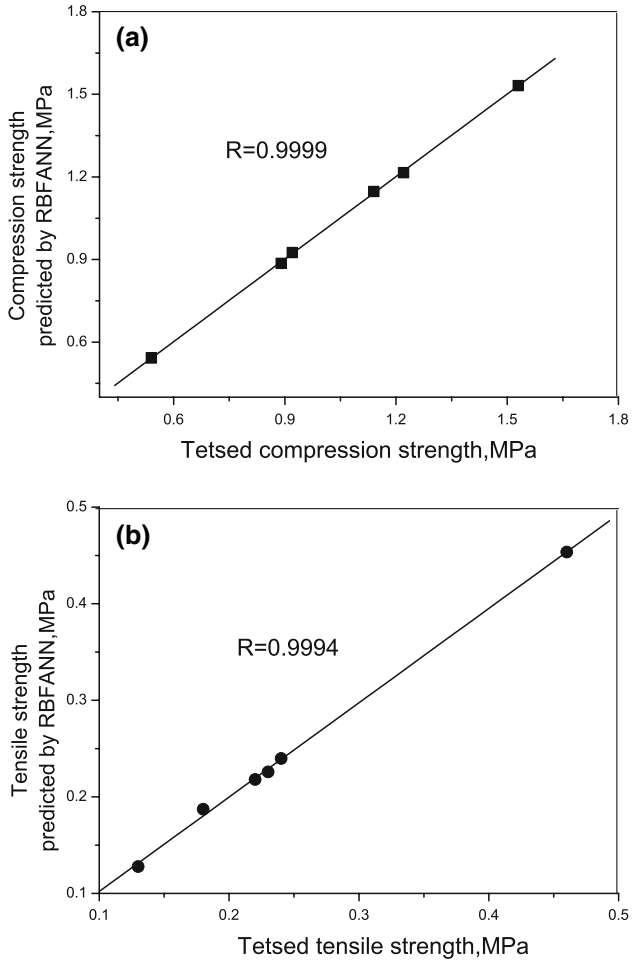

Fig. 3 The relationships between the tested parameters and corresponding values predicted by RBFANN. (a) Compression strength, (b) tensile strength

3.3 Comparison Between Afore-mentioned Two Methods

As shown in the afore-mentioned analyses for orthogonal design, the orthogonal analysis could be used to obtain the

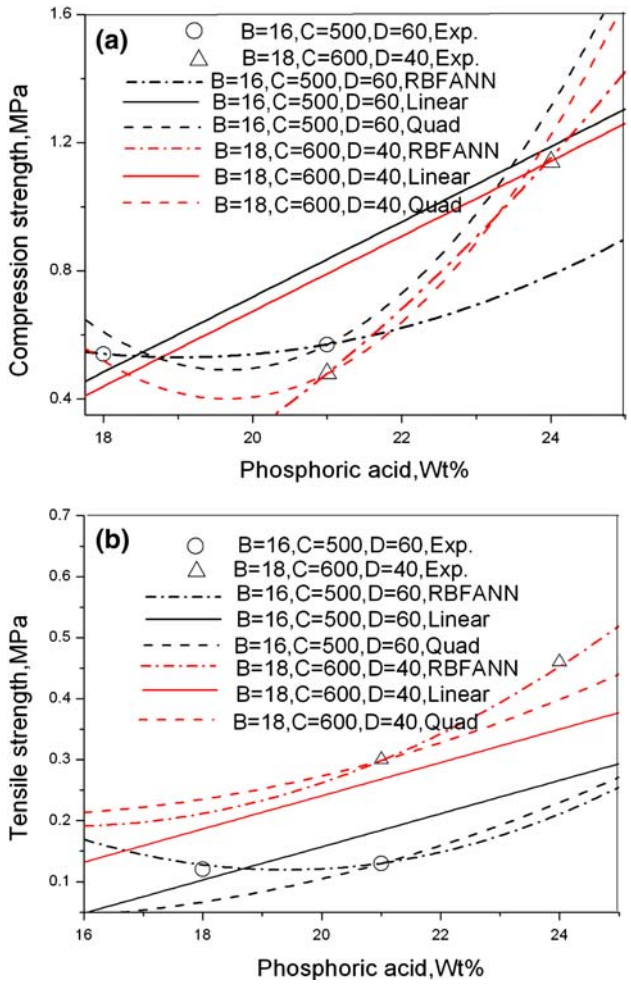

Fig. 4 The simulation results of the relationships between two parameters (the compression strength and tensile strength) and phosphoric acid by the linear regression and quadratic regression and RBFANN model when B = 16 wt.%, C = 500 °C, and D = 60 min; A = 18 wt.%, C = 600 °C, and D = 40 min, respectively

Table 8 Results of the examination test data and the predictions by Eq 3 and 4, respectively

					Compression strength, MPa			Tensile strength, MPa		
Exp. no.	*A*	*B*	*C*	*D*	Eq 3	Actual	Error, %	Eq 4	Actual	Error, %
1c	18	16	500	60	0.6096	0.54	12.9	0.8684	0.13	568.0
2c	24	18	400	80	1.4662	0.92	59.4	0.0767	0.22	–65.1
3c	21	30	600	60	0.6096	1.22	–50.0	1.6683	0.24	595.1
4c	18	16	500	80	0.9964	0.89	12.0	0.4234	0.23	84.1
5c	21	30	400	60	0.9028	1.53	–4.1	0.4683	0.18	160.2
6c	24	18	600	40	1.2228	1.14	7.3	2.1667	0.46	371.0

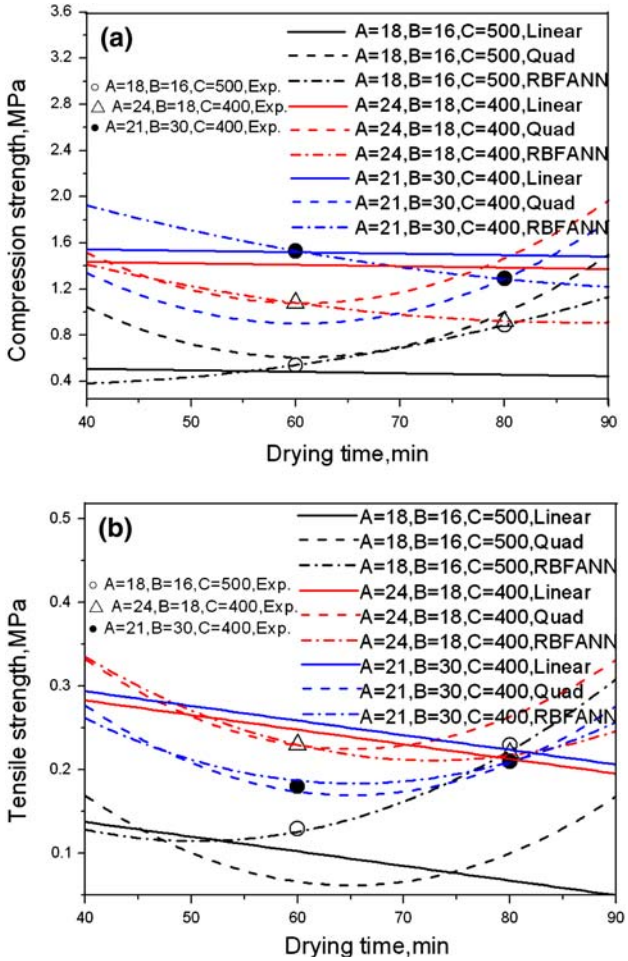

Fig. 5 The simulation results of the relationships between two parameters (the compression strength and tensile strength) and drying time by the linear regression and quadratic regression and RBFANN model when A = 18 wt.%, B = 16 wt.%, and C = 500 °C; A = 21 wt.%, B = 18 wt.%, and C = 400 °C; A = 24 wt.%, B = 30 wt.%, and C = 400 °C, respectively

optimum scheme, significance of each factor, percentage of contribution of each factor, and the linear and non-linear regressions. To investigate the prediction capacity of these linear and non-linear regressions, Table 8 shows six examination test data and the corresponding values predicted by non-linear regressions, i.e., Eq 3 and 4, respectively. From the analysis of Table 8, one can observe that the maximum errors are 59.4% for compression strength and 595.1% for the tensile strength, respectively. Therefore, one can consider that Eq 3 and 4 do not correlate the evolution of the compression strength and the tensile strength with the phosphoric acid, Al_2O_3, drying temperature, and drying time. Nevertheless, the maximum errors of RBFANN models are 0.66% for the compression strength and 4.06% for the tensile strength, respectively. Obviously, the prediction capacity of the RBFANN model is better than that of Eq 3 and 4. In addition, Fig. 4 shows the simulation results of the relationships between two parameters (the compression strength and tensile strength) and phosphoric acid by the linear regression and quadratic regression and RBFANN model when B = 16 wt.%, C = 500 °C, and D = 60 min; B = 18 wt.%, C = 600 °C, and D = 40 min, respectively. Figure 5 shows the simulation results of the relationships between two parameters (the compression strength and tensile strength) and drying time by the linear regression and quadratic regression and RBFANN model when A = 18 wt.%, B = 16 wt.%, and C = 500 °C; A = 21 wt.%, B = 18 wt.%, and C = 400 °C; A = 24 wt.%, B = 30 wt.%, and C = 400 °C, respectively. From the analysis of Fig 4 and 5, although the simulation results of the linear regression are in according with the experimental data when A = 24 wt.%, B = 18 wt.%, and C = 400 °C, other simulation results are largely different from the experimental values. In addition, the simulation results of the quadratic regressions are in agreement with the experimental data when B = 18 wt.%, C = 600 °C, and D = 40 min, A = 18 wt.%, B = 16 wt.%, and C = 500 °C, and A = 21 wt.%, B = 18 wt.%, and C = 400 °C; however, other simulation results deviate from the experimental values. Nevertheless, the simulation results of the RBFANN models are in better agreement with the experimental results under any conditions. It indicates that the RBFANN outperforms the traditional regression method.

4. Conclusions

By using the orthogonal design, Fuzzy optimum design, and artificial neural network modeling technique in present work, the following summary and conclusions can be made. The optimum composition and technology for phosphate graphite sand designed by us is phosphoric acid 24%, Al_2O_3 30%, drying temperature 400 °C, and drying time 60 min. The analysis of variance indicates that ascending sequence of the effect of four factors on both compression strength and tensile strength of phosphate graphite sand is drying time, drying temperature, Al_2O_3, and phosphoric acid. The theoretical optimum values for compression strength and tensile strength are 2.22 MPa and 0.47 MPa, respectively.

Poor prediction and simulation results of linear and quadratic regressive models for the compression strength and tensile strength by orthogonal analysis indicate that the relationships between four factors (phosphoric acid, Al_2O_3, drying temperature, and drying time) and two parameters of performance (the compression strength and tensile strength) are more complex, respectively. However, the prediction and simulation results of the RBFANN models are in better agreement with the corresponding tested values. It indicates that the RBFANN can be used to establish reliable model.

Acknowledgments

The project is supported by Science Research Fund of Hunan Provincial Education Department (06B038, 05A055), National Science Foundation of China (50774034), Science Research Fund of Hunan Provincial (06JJ20005), and Instructional Research and Reform Fund of Hunan Institute of Science and Technology (2007B06).

References

1. W. Bo-kang, C. Qi-zhou, and L. Han-tong, The Characteristics of Cryp to-crystaline Graphite Sand and its Application in Al-alloy Castings, *Foundry (in Chinese)*, 1997, **47**(7), p 1–5

2. S. Gui-qiao, X. Hua-sheng, and Z. Chun-hui, Study on Infrared Preheating Process of Graphic Mould for Thin-walled Titanium-alloy Casting, *Foundry (in Chinese)*, 2004, **53**(3), p 194–196
3. P. Ye, Z. Chuan, Z. Yan-cheng, and S. Guo-xiong, Fabrication of Al_2O_3 Ceramic Matrix Composites and their Microstructure, *Special Casting Nonferrous Alloys (in Chinese)*, 2005, **25**(6), p 347–349
4. J. Paulo Davim, Design of Optimisation of Cutting parameters for Turning Metal Matrix Composites Based on the Orthogonal Arrays, *J. Mater. Process. Technol.*, 2003, **132**, p 340–344
5. J. Paulo Davim, An Experimental Study of the Tribological Behavior of the Brass/Steel Pair, *J. Mater. Process. Technol.*, 2000, **100**, p 273–277
6. E. Bagci and S. Aykut, A Study of Taguchi Optimization Method for Identifying Optimum Surface Roughness in CNC Face Milling of Cobalt-based Alloy (Stellite 6), *Int. J. Adv. Manuf. Technol.*, 2006, **29**, p 940–947
7. Y.-Z. Fan, Y.-Y. Wang, P.-Y. Qian, and J.-D. Gu, Optimization of Phthalic Acid Batch Biodegradation and the Use of Modified Richards Model for Modelling Degradation, *Int. Biodeterior. Biodegrad.*, 2004, **53**, p 57–63
8. C.C. Tsao, Taguchi Analysis of Drilling Quality Associated with Core Drill in Drilling of Composite Material, *Int. J. Adv. Manuf. Technol.*, 2007, **32**, p 877–884
9. J.-R. Shie, Optimization of Dry Machining Parameters for High-Purity Graphite in End-Milling Process by Artificial Neural Networks: A Case Study, *Mater. Manuf. Processes*, 2006, **21**, p 838–845
10. J. Sheikh-Ahmand and J. Twomey, ANN Constitutive Model for High Strain-rate Deformation of Al 7075-T6, *J. Mater. Process. Technol.*, 2007, **186**, p 339–345
11. A. Dharia and H. Adeli, Neural Network Model for Rapid Forecasting of Freeway Link Travel Time, *Eng. Appl. Artif. Intell.*, 2003, **16**, p 607–613
12. L. Aijun, L. Hejun, L. Kezhi, and G. Zhengbing, Applications of Neural Networks and Genetic Algorithms to CVI Processes in Carbon/Carbon Composites, *Acta Mater.*, 2004, **52**, p 299–305
13. G. Serpen and Y.F. Xu, Simultaneous Recurrent Neural Network Trained with Non-recurrent Backpropagation Algorithm for Static Optimization, *Neural Comput. Appl.*, 2003, **12**, p 1–9
14. K.G. Keong, W. Sha, and S. Malinov, Artificial Neural Network Modelling of Crystallization Temperatures of the Ni–P Based Amorphous Alloys, *Mater. Sci. Eng. A*, 2004, **365**, p 212–218
15. M. Sen and H.S. Shan, Optimal Selection of Machining Conditions in the Electrojet Drilling Process Using Hybrid NN-DF-GA Approach, *Mater. Manuf. Processes*, 2006, **21**, p 349–356
16. H. Saxén and F. Gunturu, Evolving Nonlinear Time-Series Models of the Hot Metal Silicon Content in the Blast Furnace, *Mater. Manuf. Processes*, 2007, **22**, p 577–584